Ab initio potential-energy surface of LiH_2^+ and its analytical representation

D. J. Searles and E. I. von Nagy-Felsobuki*
Department of Chemistry, University of Newcastle, Newcastle, New South Wales 2308, Australia
(Received 21 May 1990; revised manuscript received 1 October 1990)

A 170-point configuration-interaction involving all single and double excitations *ab initio* potential-energy surface for the LiH_2^+ molecule was calculated using $(11s3p1d)/[6s3p1d]$ and $(8s3p1d)/[6s3p1d]$ contracted Gaussian basis sets for lithium and hydrogen, respectively. Various analytical functions were tested as representations of the discrete surface. A Padé-approximant function with a Dunham expansion variable was found to give the most reliable representation with a χ^2 of 1.3×10^{-7}. It is this surface that is recommended for rovibrational calculations.

I. INTRODUCTION

Traditionally, studies of vibrational and rotational inelastic scattering by the energy-change methods have employed ions as they are more easily energy selected and analyzed than neutral species and can be detected with high efficiency. Due to its electronic simplicity, many studies have centered on unravelling the scattering collisions of Li^+ on H_2.[1–5] For example, Toennies and coworkers[1–3] in 1973 reported measurement of differential cross sections for resolved vibrational transitions at center-of-mass collision energies ($E_{c.m.}$) between 2 and 9 eV and in 1979 detailed measurements of rotationally inelastic scattering for $E_{c.m.}$ at 0.6 eV.

Theoretical studies[6–19] have consistently predicted that the LiH_2^+ ion possesses C_{2v} symmetry. The interaction between H_2 and Li^+ is found to be highly anisotropic and the approach of Li^+ ion to the H_2 molecule strongly influences the behavior of the potential-energy curve at the equilibrium distance. The more sophisticated calculations[8–11,15–18] have predicted that the ion possesses a small binding energy of between 20 and 25 $kJ\,mol^{-1}$ with respect to $Li^+ + H_2$ (which has been confirmed by experiment[20]). These predictions are consistent with the view that the LiH_2^+ ion is a weak complex between a hydrogen molecule and the Li^+ ion.

In the early 1970s Lester[8,9] calculated a 150-point Hartree-Fock self-consistent-field (HF-SCF) potential-energy surface of LiH_2^+. As is well known, the HF method does not take into consideration electron correlation, with the exception of the exchange term. Hence, accurate HF wave functions account for ~99.5% of the absolute energy of a molecule.[11] Nevertheless, as the other 0.5% is greater than the experimental binding energy of LiH_2^+, the absence of correlation corrections requires essentially complete cancellation of the correlation effects between products(s) and reactant(s) along any dissociative channel in order for the HF potential to be realistic well away from the minimum-energy geometry. It is argued that the HF potential is a "good" approximation for this collision complex, since the number of paired electrons is the same in the products ($Li^+ + H_2$) as in the reactant (LiH_2^+).[8,9,11] However, as Kutzelnigg, Staemmler, and Hoheisel[10] (KSH) have pointed out, for collinear Li^+-H_2 collisions intra-H_2 correlation is far from constant over a range of geometries and, furthermore, for perpendicular collisions it has a minimum for geometries close to the minimum C_{2v} geometry. The conclusion drawn by KSH (Ref. 10) is that Lester's SCF surface is poorly described where dissociative collisions are possible. Nevertheless, recently Russek, Snyder, and Furlan[19] have calculated a ~120-point HF-SCF surface for their classical trajectory studies in which the scattering angles were in excess of a few tenths of a degree, in order to model the vibrotational energy in the Li^+-D_2 collision complex.

In 1973 KSH (Ref. 10) computed a HF-SCF and a PNO (paired natural orbitals) -IEPA (independent electron pair approximation) potential-energy surface. Each surface consisted of over 300 points. Unfortunately the IEPA is not variational and so calculated pair-correlation energies may be well in excess of CISD (configuration interaction involving all single and double excitations from a single HF reference determinant) correlation energies obtained using the same basis set.[21–22] This has been ascribed to the fact the IEPA ignores matrix elements between configurations belonging to different pairs and so it tends to overestimate the correlation energy when several orbitals occupy the same region of space.[22] That is, the method may lead to a positive or negative error in the total energy.

The only CISD calculation of LiH_2^+ in the literature is that of Dixon, Gole, and Komornicki.[18] In calculating the Li^+ affinity of H_2 they showed that the second-order Moller-Plesset perturbation method (MP2) energies are in excellent agreement with the CISD calculations near the minimum geometry.

Quasiclassical, semiclassical, and approximate quantal scattering calculations have relied heavily on Lester's HF-SCF and the PNO-IEPA potential-energy surfaces. Comparisons of experimental with theoretical differential cross sections and transition probabilities due to rotationally inelastic scattering at 0.6 eV have been made in order to test the accuracy of *ab initio* methods.[2,3,23–25] These studies have shown that the experimental differential cross sections are qualitatively in agreement. However, they have been angularly shifted with respect to the

theoretical result. Difficulties have also been encountered in reproducing vibrational transition probabilities in detail.[4] It is unclear whether the inadequacy is with the *ab initio* potential-energy surfaces or with failures due to the dynamic approximations.[3,4]

At present, Legendre expansions are generally used to represent the potential-energy surface for scattering calculations. This greatly facilitates the evaluation of coupling matrix elements for rotational (with vibrational) energy transfer.[26] However, in the case of rovibrational calculations, a variety of analytical representations can be employed.[27–34]

It is the purpose of this paper to detail a CISD potential-energy surface of LiH_2^+ and its analytical representation, based upon a strategy developed by von Nagy-Felsobuki and co-workers in order to calculate the vibrational band origins of H_3^+ (Refs. 27-31) and Li_3^+ (Refs. 32-34). The surface and its analytical representation differ in a number of aspects from those already reported in the literature.[8–10,19] First, the Cl methodology is variational and so is an upper bound to the "exact" energy. Second, a vibrational coordinate space[35] for the discrete surface is used and generated by a quadrature scheme proposed by Harris, Engerholm, and Gwinn.[36] Third, in order to assist rovibrational calculations the coordinate space is restricted to the small r_{Li-x} (where x is the center of the H—H bond), small r_{H-H}, and $0 \le \vartheta \le 90$ (where ϑ is the angle between the vectors $\mathbf{r}_{Li-x}$ and $\mathbf{r}_{H-H}$). Hence we are sampling the potential-energy surface at the region where a three-term Legendre expansion may not be justified and where the approach of the Li^+ ion to the H_2 molecule strongly influences the behavior of the potential curve of the complex.

II. DISCRETE CISD SURFACE

We have adopted the CISD ansatz (including size correction) embedded in the GAUSSIAN 86 suite of programs.[37] For electronic calculations we have employed the $(11s3p1d)/[6s3p1d]$ lithium basis of Gerber and Schumacher[38] with the d exponent being 0.15 and the $(8s3p1d)/[6s3p1d]$ hydrogen basis of Dykstra and Swope.[39] This compares favorably to the $(9s3p)/[5s3p]$ lithium and $(6s3p)$ hydrogen basis used by Lester[8,9] and the Gaussian lobe basis $(9s4p)/[6s4p]$ for lithium and $(5s3p)/[3s3p]$ hydrogen basis used by KSH.[10] It should be noted that in addition to the nuclear centered lobe functions KSH[10] employed p-type bond functions which in hindsight they concluded, "...improves the energy for intermediate H-H distances but is less effective or has even the opposite effect for very large or very small distances."

Table I compares the CISD and PNO-IEPA energies for H_2 with the exact results calculated by Kolos and Wolniewicz.[40] It is clear that not only are each of the CISD calculated points more accurate than the PNO-IEPA calculations but the CISD points parallel the exact surface far more closely (with an error of 0.001 E_h for the CISD calculations compared to $0.003-0.006E_h$ for the PNO-IEPA calculations). Table I also highlights the problems with employing a nonvariational methodology in constructing a potential-energy surface. At a distance of $1.2a_0$ the PNO-IEPA methodology gives a spurious energy (i.e., $\sim 0.003E_h$ lower than the exact result). This brings into question the correlation energy calculated by the PNO-IEPA methodology at various points of the energy hypersurface of Li^+-H_2.

The exact HF energy of the Li^+ ion is $-7.236\,41E_h$,[41] whereas our lithium basis yields $-7.236\,21E_h$, a difference of only $0.0002E_h$. On the other hand, both Lester[9] and KSH (Ref. 10) obtained SCF energies $0.0004E_h$ higher than the exact HF value. Interestingly, our CISD energy is $0.02E_h$ lower than our SCF energy, whereas in the case of H_2 the difference is $0.04E_h$ at an r_{H-H} distance of $1.4a_0$. Hence, the exclusion of correlation effects would yield incorrect relative energies for the LiH_2^+ molecule and the disociated Li^+-H_2.

Ab initio investigations have consistently predicted the LiH_2^+ molecule to have C_{2v} symmetry. The predicted equilibrium geometries and minimum potential energies (E_0) using various basis sets and methodologies are presented in Table II. Our HF optimization gives an E_0 energy of $-8.378\,902\ E_h$ for the C_{2v} geometry, with a r_{Li-H} separation of $3.893\ a_0$ and a θ_{H-Li-H} bond angle of 20.8°. Our calculated HF E_0 is the lowest so far reported in the literature (as is illustrated in Table II) thereby vindicating the size of the basis set employed. The respective CISD calculations also gave the lowest variational Cl energy, with a predicted geometry not greatly dissimilar to our HF geometry (i.e., C_{2v} geometry with an r_{Li-H} separation of $3.860a_0$ and a θ_{H-Li-H} bond angle of

TABLE I. Comparison of Cl energies for H_2. (All energies in Hartrees. The symbol Δ represents the difference between exact and calculated energies.)

r_{H-H}/a_0	Exact[a]	This work CISD (Δ)	PNO-IEPA (Δ)[b]
1.0	−1.124 54	−1.123 24(0.001 30)	−1.119 90(0.004 64)
1.2	−1.164 93	−1.163 79(0.001 14)	−1.167 97(−0.003 04)
1.4	−1.174 47	−1.173 39(0.001 08)	−1.170 90(0.003 57)
1.8	−1.155 07	−1.153 94(0.001 13)	−1.151 73(0.003 34)
2.4	−1.102 42	−1.101 10(0.001 32)	−1.098 51(0.003 91)
3.0	−1.057 32	−1.055 98(0.001 34)	−1.051 67(0.005 65)

[a]See Ref. 40.
[b]See Ref. 10.

21.2°).

The CISD calculations indicate that LiH_2^+ is weakly bound with respect to $Li^+ + H_2$ by 24.9 kJ mol^{-1}. This compares favorably to the experimental value of 27.2 kJ mol^{-1} (Ref. 20) and with other theoretically calculated values of 21.8 (SCF),[11] 23.4 (MP2),[15] 23.1 (SCF),[17] 21.3 (CISD),[18] and 21.5 kJ mol^{-1} (MP2).[18]

The discrete CISD potential-energy surface consists of energies at 170 geometries with a maximum energy of $-7.675\,238\ E_h$.[42] An initial set of 39 points was calculated along the vibrational or displacement t coordinates (for a C_{2v} triatomic) as derived by Carney, Langhoff, and Curtiss.[35] The t coordinates are described in Fig. 1 and are related to the three bond lengths via

$$r_{12}=\left\{\left[-Ra-\frac{\lambda}{M_{\mathrm{H}}}\left[\frac{b}{\gamma}t_1+\frac{b\alpha}{\mu\gamma}t_1-bt_2-at_3\right]+\frac{2\lambda}{m_{\mathrm{Li}}}\left[\frac{-b}{\gamma}t_1-\frac{b\alpha}{\mu\gamma}t_1+bt_2\right]\right]^2 + \left[Rb-\frac{2\lambda}{m_{\mathrm{Li}}}bt_3-\frac{\lambda}{m_{\mathrm{H}}}\left[\frac{-a}{\gamma}t_1-\frac{a\alpha}{\mu\gamma}t_1+at_2+bt_3\right]\right]^2\right\}^{1/2}, \tag{1}$$

$$r_{23}=\left\{\left[Ra+\frac{\lambda}{m_{\mathrm{H}}}\left[\frac{b}{\gamma}t_1+\frac{b\alpha}{\mu\gamma}t_1-bt_2+at_3\right]-\frac{2\lambda}{m_{\mathrm{Li}}}\left[\frac{-b}{\gamma}t_1-\frac{b\alpha}{\mu\gamma}t_1+bt_2\right]\right]^2 + \left[Rb+\frac{2\lambda}{m_{\mathrm{Li}}}bt_3+\frac{\lambda}{m_{\mathrm{H}}}\left[\frac{a}{\gamma}t_1-\frac{a\alpha}{\mu\gamma}t_1+at_2+bt_3\right]\right]^2\right\}^{1/2}, \tag{2}$$

$$r_{13}=\left\{\left[2Rb+\frac{2\lambda}{m_{\mathrm{H}}}\left[\frac{a}{\gamma}t_1\right]\right]^2+\left[\frac{2\lambda}{m_{\mathrm{H}}}at_3\right]^2\right\}^{1/2}, \tag{3}$$

where

$$a=\cos\frac{\theta}{2},\quad b=\sin\frac{\theta}{2},\quad \lambda=\left[\frac{2}{m_{\mathrm{Li}}^2}+\frac{4b^2}{m_{\mathrm{H}}^2}\right]^{-1/2},$$

$$\mu=\lambda^2\left[\frac{2}{m_{\mathrm{Li}}}+\frac{4b^2}{m_{\mathrm{H}}}\right],\quad \alpha=\lambda^2\left[\frac{2\cos\theta}{m_{\mathrm{Li}}}-\frac{4b^2}{m_{\mathrm{H}}}\right],\quad \gamma=\left[1-\frac{\alpha^2}{\mu^2}\right]^{1/2}.$$

TABLE II. Comparison of *ab initio* results for LiH_2^+.

Reference	Method	Li basis	H basis	$r_{\text{Li-H}}/a_0$	θ (deg)	E_0/E_h
6	DIM			5.0	16.1	a
7	FSGF	(2*s*)		3.436	25.3	−6.920
8-9	HF	(9*s*3*p*)/[5*s*3*p*]	(6*s*3*p*)	3.83	21.1	−8.3783
10	HF	(9*s*4*p*)/[6*s*4*p*]	(5*s*3*p*)/[3*s*3*p*]	3.81	21.1	−8.3782
	PNO-IEPA	(9*s*4*p*)/[6*s*4*p*]	(5*s*3*p*)/[3*s*3*p*]	3.81	21.1	−8.4560
11	HF	(8*s*5*p*)	(6*s*4*p*)	3.975	20.4	−8.3744
13	HF	4-31*G*		4.269	18.7	−8.3645
	MP2[b]	6-31*G***		4.269	18.7	−8.4007
14	FSGF	(2*s*)		3.97	20.3	−6.9201
15	HF[c]	6-311*G*(2*d*,2*p*)		4.050	19.9	−8.3777
	MP2	6-311*G*(2*d*,2*p*)		4.050	19.9	−8.4200
16	HF	6-31*G***		4.06	19.5	−8.3682
	SCEP[b]	6-31*G***		4.06	19.5	−8.4079
17	HF	(9*s*5*p*)	(9*s*5*p*)	3.872	21.0	−8.3787
18	HF	(11*s*4*p*2*d*)/[5*s*2*p*1*d*]	(5*s*2*p*)/[3*s*2*p*]	3.957	20.4	−8.3775
	CISD[b]	(11*s*4*p*2*d*)/[5*s*2*p*1*d*]	(5*s*2*p*)/[3*s*2*p*]	3.957	20.4	−8.4151
	MP2[b]	(11*s*4*p*2*d*)/[5*s*2*p*1*d*]	(5*s*2*p*)/[3*s*2*p*]	3.957	20.4	−8.4071
This work	HF	(11*s*3*p*1*d*)/[6*s*3*p*1*d*]	(8*s*3*p*1*d*)/[6*s*3*p*1*d*]	3.893	20.8	−8.3789
	CISD	(11*s*3*p*1*d*)/[6*s*3*p*1*d*]	(8*s*3*p*1*d*)/[6*s*3*p*1*d*]	3.860	21.2	−8.4351

[a]Predicted binding energy with respect to $Li^+ + H_2$ is 10.5 kJ mol^{-1}.
[b]Single-point calculation at optimized HF geometry.
[c]Single-point calculation at the MP2 optimized geometry.

In the first instance, the diagonal points in the t coordinates were fitted with a fifth-order exponential power series. The resulting fit was then used with the quadrature scheme of Harris, Engerholm, and Gwinn[36] to generate additional points in the t-coordinate space. Generally such a strategy gives a greater density of points where the potential surface is shallow, therefore ensuring that the succeeding fits are properly weighted by data points in the more difficult regions on the potential-energy surface. In our scheme we obtain $20\times20\times20$ quadrature points which are too numerous to keep the problem tractable. Hence using graphical inspections, the additional 8000 t-coordinate points are culled to 70 points, giving 109 points in total. Each of these points corresponds to a C_{2v} configuration of LiH_2^+. The Li-H separation ranges from 1.722 739 to 7.791 276 a_0 while the H-H separation ranges from 0.654 159 to 5.894 657a_0.

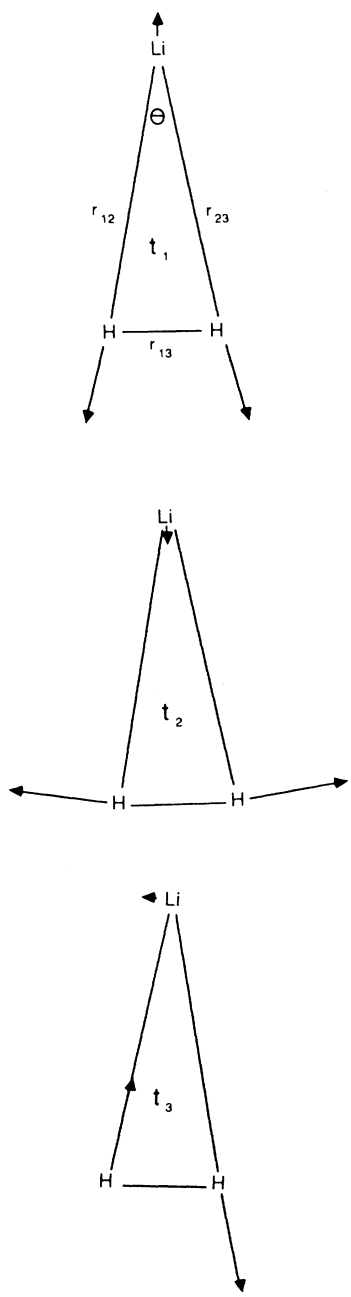

FIG. 1. The t-vibrational modes as defined by Eqs. 1–3.

The t coordinates are only appropriate for a C_{2v} geometry and so an additional 61 collinear points [with the atoms in the configuration $(\text{Li-H-H})^+$] were calculated between $1.0\le r_{\text{H-H}}\le 3.0$ and $0.95\le r_{\text{Li-H}}\le 4.0$, where H represents the nearest hydrogen nucleus to lithium.

An important feature of the discrete surface is the saddle point corresponding to the linear $(\text{Li-H-H})^+$ form of the molecule. A CISD optimization was used to determine the minimum-energy collinear geometry. The collinear minimum has an energy of $-8.428142E_h$ for a Li-H separation of $3.870a_0$ and a H-H separation of $1.402a_0$. This geometry has an energy only 18 kJ mol^{-1} above that of the equilibrium C_{2v} structure. A stationary point is also observed for the linear $(\text{H-Li-H})^+$ configuration. However, it has a relatively high energy barrier (224 kJ mol^{-1}) with a Li-H separation of $4.239a_0$.

III. ANALYTICAL REPRESENTATION

Lester[8,9] and KSH (Ref. 10) developed intermolecular analytical representations for their respective discrete potential-energy surfaces. For example, KSH (Ref. 10) developed a five-term exponential series expansion in $r_{\text{H-H}}$ with the angular dependence generated by a three-term Legendre expansion. This intermolecular approach is desirable for the Li^+-ion distant from the H_2 molecule, since it is easy to incorporate the monopole-quadrupole interaction term(s). The Legendre is commonly used in the scattering calculations since it simplifies the potential-energy integrals involved in the calculation of scattering properties.[26]

For geometries concomitant with the bonding nature of the LiH_2^+ molecular ion and its vibrational excitation, where Li^+-H_2 distances are small, a three-term Legendre expansion may not be justified.[10] It is then desirable to develop an analytical representation following the guidelines suggested by Burton *et al.*[29] Consequently, for H_3^+ (Refs. 27-31) and Li_3^+ (Refs. 32-34) power-series expansions of Dunham,[43] Simons, Parr, and Finlan,[44] and Ogilvie[45] and the Morse-type variants were examined in detail.[33]

Of all the possible power-series variants investigated previously the Morse-Dunham and Ogilvie expansions most accurately reproduce the LiH_2^+ discrete surface. The Morse-Dunham expansion variable has the form

$$\rho_i = 1-\exp\left[\frac{-(r_i-r_e)}{r_e}\right], \tag{4}$$

where ρ_i is the internuclear separation of two atoms and r_e is their separation when the molecule is at its equilibrium geometry. The Ogilvie expansion variable has the form

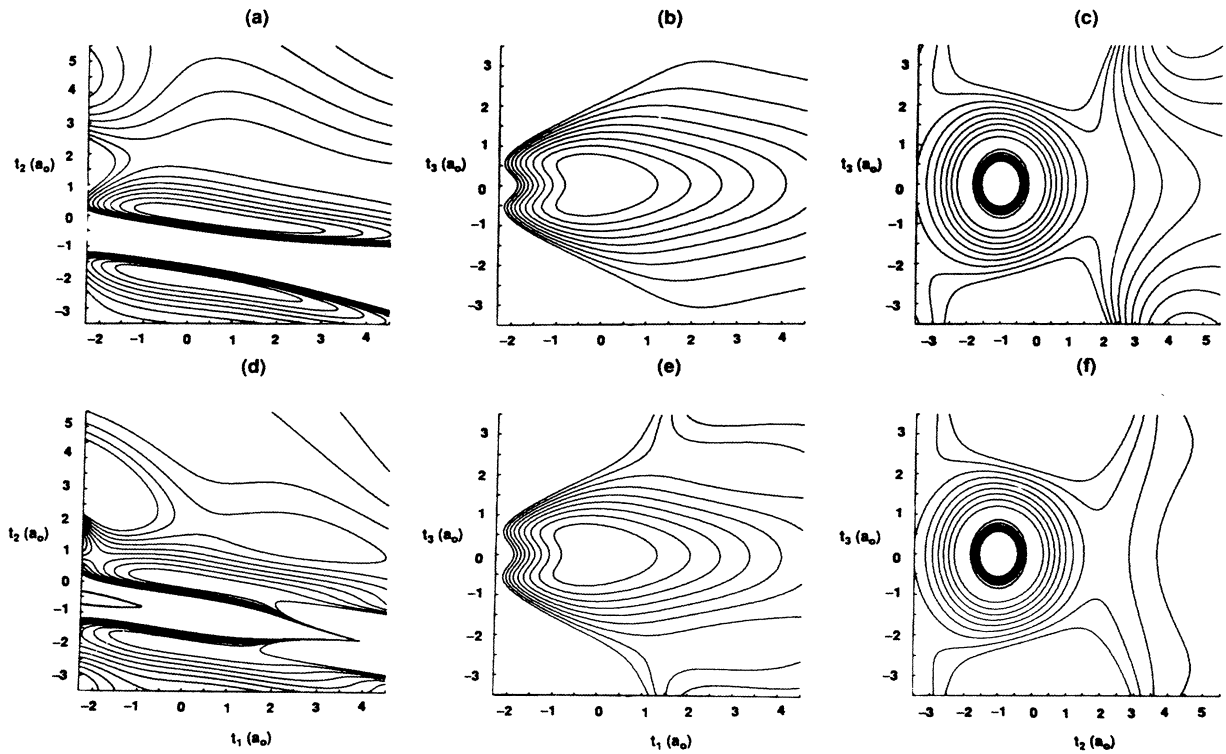

FIG. 2. Ogilvie and Morse-Dunham contour plots for the LiH_2^+ potential-energy surface. Contours are in increments of 50 kJ mol^{-1}. (a) t_1-t_2 sixth-order Ogilvie-type fit. (b) t_1-t_3 sixth-order Ogilvie-type fit. (c) t_2-t_3 sixth order Ogilvie-type fit. (d) t_1-t_2 sixth-order Morse-Dunham-type fit. (e) t_1-t_3 sixth-order Morse-Dunham-type fit. (f) t_2-t_3 sixth-order Morse-Dunham-type fit.

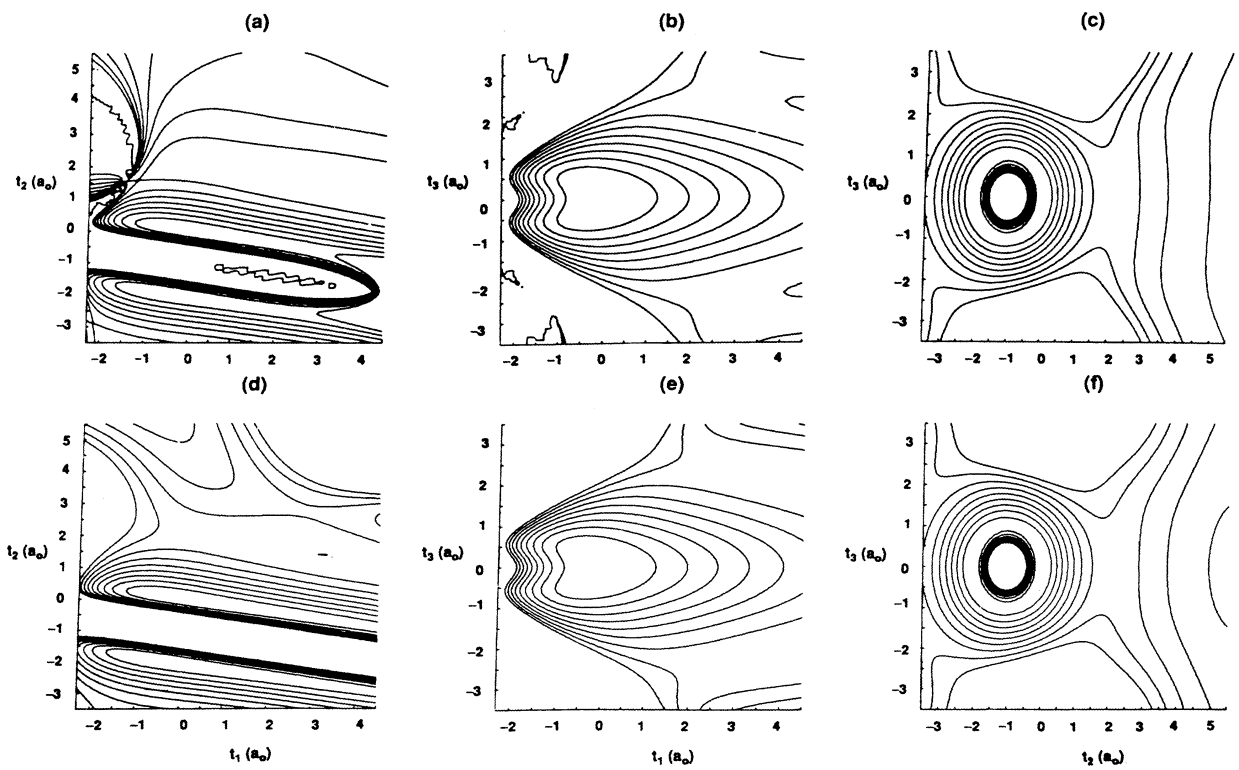

FIG. 3. Padé-approximant contour plots for the LiH_2^+ potential-energy surface. Contours are in increments of 50 kJ mol^{-1}. (a) t_1-t_2 Padé (6,6) -type fit. (b) t_1-t_3 Padé (6,6) -type fit. (c) t_2-t_3 Padé (6,6) -type fit. (d) t_1-t_2 Padé (6,4) -type fit. (e) t_1-t_3 Padé (6,4) -type fit. (f) t_2-t_3 Padé (6,4) -type fit.

TABLE III. Expansion coefficients for Dunham-Padé–Approximant expansion of the LiH_2^+ potential-energy surface.

Term	Expansion parameter	Expansion coefficient Numerator	Expansion coefficient Denominator
	1	−178.2047	−1.000 00
1	$\rho_1+\rho_2$	−336.4846	−0.888 19
2	ρ_3	−161.7542	0.092 31
3	$\rho_1^2+\rho_2^2$	−208.6695	−0.293 81
4	ρ_3^2	41.8770	0.100 78
5	$\rho_1\rho_2$	−695.5297	−1.116 38
6	$\rho_2\rho_3+\rho_1\rho_3$	−292.5161	0.155 11
7	$\rho_1^3+\rho_2^3$	−94.2672	−0.233 76
8	ρ_3^3	2.0409	−0.059 72
9	$\rho_1^2\rho_2+\rho_2^2\rho_1$	−354.4265	0.306 68
10	$\rho_1^2\rho_3+\rho_2^2\rho_3$	−157.0927	0.137 08
11	$\rho_1\rho_3^2+\rho_2\rho_3^2$	98.3250	0.125 34
12	$\rho_1\rho_2\rho_3$	−681.6319	−0.336 84
13	$\rho_1^4+\rho_2^4$	−43.3469	−0.017 44
14	ρ_3^4	−8.8394	0.000 66
15	$\rho_1^3\rho_2+\rho_2^3\rho_1$	−39.7770	0.000 52
16	$\rho_1^3\rho_3+\rho_2^3\rho_3$	−66.8614	0.024 61
17	$\rho_1\rho_3^3+\rho_2\rho_3^3$	18.4490	−0.002 95
18	$\rho_1^2\rho_2^2$	−89.4748	0.004 43
19	$\rho_1^2\rho_3^2+\rho_2^2\rho_3^2$	81.1499	−0.008 74
20	$\rho_1^2\rho_2\rho_3+\rho_1\rho_2^2\rho_3$	−360.3963	0.002 58
21	$\rho_1\rho_2\rho_3^2$	106.3896	0.002 59
22	$\rho_1^5+\rho_2^5$	−2.9803	
23	ρ_3^5	−0.1271	
24	$\rho_1^4\rho_2+\rho_2^4\rho_1$	−46.0157	
25	$\rho_1^4\rho_3+\rho_2^4\rho_3$	−38.8884	
26	$\rho_1\rho_3^4+\rho_2\rho_3^4$	−7.8769	
27	$\rho_1^3\rho_2^2+\rho_1^2\rho_2^3$	56.0775	
28	$\rho_1^3\rho_3^2+\rho_2^3\rho_3^2$	30.0708	
29	$\rho_1^2\rho_3^3+\rho_2^2\rho_3^3$	13.0266	
30	$\rho_1^3\rho_2\rho_3+\rho_1\rho_2^3\rho_3$	−12.3412	
31	$\rho_1\rho_2\rho_3^3$	30.9005	
32	$\rho_1^2\rho_2^2\rho_3$	−145.8230	
33	$\rho_1^2\rho_2\rho_3^2+\rho_1\rho_2^2\rho_3^2$	30.9203	
34	$\rho_1^6+\rho_2^6$	−1.5057	
35	ρ_3^6	0.0213	
36	$\rho_1^5\rho_2+\rho_2^5\rho_1$	−0.8166	
37	$\rho_1^5\rho_3+\rho_2^5\rho_3$	−2.3367	
38	$\rho_1\rho_3^5+\rho_2\rho_3^5$	−0.3036	
39	$\rho_1^4\rho_2^2+\rho_2^4\rho_1^2$	−2.4217	
40	$\rho_1^4\rho_3^2+\rho_2^4\rho_3^2$	4.4660	
41	$\rho_1^2\rho_3^4+\rho_2^2\rho_3^4$	1.2108	
42	$\rho_1^4\rho_2\rho_3+\rho_2^4\rho_1\rho_3$	−37.2704	
43	$\rho_1\rho_2\rho_3^4$	−7.0436	
44	$\rho_1^3\rho_2^3$	5.8807	
45	$\rho_1^3\rho_3^3+\rho_2^3\rho_3^3$	−3.2093	
46	$\rho_1^3\rho_2^2\rho_3+\rho_1^2\rho_2^3\rho_3$	51.3713	
47	$\rho_1^3\rho_2\rho_3^2+\rho_1\rho_2^3\rho_3^2$	28.0094	
48	$\rho_1^2\rho_2\rho_3^3+\rho_1\rho_2^2\rho_3^3$	11.7577	
49	$\rho_1^2\rho_2^2\rho_3^2$	−51.1058	
χ^2		1.3×10^{-7}	

$$\rho_i=\frac{2(r_i-r_e)}{(r_i+r_e)} . \tag{5}$$

The sixth-order Morse-Dunham–type and the Ogilvie-type expansion variables give the smallest sum of squares of residuals. In particular, the χ^2 for the sixth-order Morse-Dunham and the sixth-order Ogilvie are 1.4×10^{-4} and 4.5×10^{-5}, respectively.

Figures 2(a)–2(c) show energy contour plots using the sixth-order Ogilvie fit, whereas Figs. 2(d)–2(f) show energy contour plots using the sixth-order Morse-Dunham fit to represent the discrete surface. In all figures each contour represents an energy increment of 50 kJ mol^{-1} (with approximately 2.5 kJ mol^{-1} available from ambient surroundings).

Unlike the sixth-order Ogilvie fit, graphical examination of the physical nature of the sixth-order Morse-Dunham fit in the region defined by the data indicates that the functions do not satisfy the criterion[29] of being smooth everywhere with monotonically increasing repulsive walls. As in the case of H_3^+ (Ref. 29) and Li_3^+ (Ref. 33), some of the high-order coefficients for this fit and the sixth order Ogilvie fit are large. Singular value decomposition (SVD) analysis on the sixth-order Ogilvie fit (setting σ_{47} to zero) yields a χ^2 of 4.8×10^{-5}, which has only marginally degraded the fit. A similar SVD analysis of the sixth-order Morse-Dunham fit did not eliminate singularities.

The χ^2 of the power series fits are too poor to be appropriate for rovibrational or scattering calculations. Consequently, investigations were conducted on the use of Padé approximants. Padé approximants have been used as analytical representations of diatomic potential-energy curves.[46–48] Padé approximants are rational functions in which the numerator and denominator are power-series expansions (of order m and n, respectively) of a variable ρ. That is,

$$P(m,n)=\frac{\sum_{i=0}^{m}\sum_{j=0}^{m}\sum_{k=0}^{m} a_{ijk}\rho_1^i\rho_2^j\rho_3^k}{-\sum_{i'=0}^{n}\sum_{j'=0}^{n}\sum_{k'=0}^{n} b_{i'j'k'}\rho_1^{i'}\rho_2^{j'}\rho_3^{k'}} , \tag{6}$$

such that $(i+j+k)\le m$ and $(i'+j'+k')\le n$.

The six variables previously used for the power-series expansions[33] were also used as expansion variables in the Padé-approximant representations. In each case, the χ^2 of the ensuing fits are lower than those for the respective power-series representations. However, on graphical examinations it was revealed that the Padé surfaces suffered from a substantial increase in the number of singularities. Moreover, the singularities are not removed by use of the SVD analysis. For example, Figs. 3(a)–3(c) give the energy contour plots with respect to t coordinates for a sixth-order Padé approximant [denoted $P(6,6)$] using Dunham expansion variables. Of all the variants, this fit gives the lowest χ^2 of 1.1×10^{-8}.

An alternative form of the Padé approximant was tested to represent the LiH_2^+ surface. It has the form

$$P'(m,n)=\frac{\sum_{i=0}^{m}\sum_{j=0}^{m}\sum_{k=0}^{m} a_{ijk}\rho_1^i\rho_2^j\rho_3^k}{r_{12}r_{23}r_{13}\left[-\sum_{i'=0}^{n}\sum_{j'=0}^{n}\sum_{k'=0}^{n} b_{i'j'k'}\rho_1^{i'}\rho_2^{j'}\rho_3^{k'}\right]} , \tag{7}$$

where $(i+j+k) \leq m$ and $(i'+j'+k') \leq n$. The two $r_{\text{Li-H}}$ separations are represented by r_{12} and r_{23} and the $r_{\text{H-H}}$ separation by r_{13}. This function gives a small χ^2 for all the variants but in general the high-order expansion coefficients are large and graphical inspections of the contour plots revealed many singularities. However, the Dunham expansion which is sixth order in the numerator and fourth order in the denominator [that is, $P'(6,4)$] gives a function that is smooth and has monotonically increasing repulsive walls over the region defined by the data points. The fit gives a χ^2 of 1.3×10^{-7}, which indicates that this fit is substantially more accurate than the best power-series expansion. Contour plots for this surface are given in Figs. 3(d)–3(f) and the expansion coefficients of the $P'(6,4)$ Padé approximant are given in Table III. It is this surface that is recommended to be used in calculations involving rovibrational properties.[19,29–34]

ACKNOWLEDGMENTS

Calculations were performed using the VAX 8550s, VAX 3100 workstation, and Cray-XMP; the former made available via the generous support of the Computing Center University of Newcastle and the latter by generous support of Leading Edge Technologies, Ltd. We also wish to acknowledge the support of the Australian Grants Scheme, AINSE, and the Senate Research Committee, University of Newcastle.

*Author to whom correspondence should be addressed.

[1]R. David, M. Faubel, and J. P. Toennies, Chem. Phys. Lett. **18**, 87 (1973).

[2]G. D. Barg, G. M. Kendall, and J. P. Toennies, Chem. Phys. **16**, 243 (1976).

[3]M. Faubel and J. P. Toennies, J. Chem. Phys. **71**, 3770 (1979).

[4]D. J. Krajnovich, C. S. Parmenter, and D. L. Catlett, Jr., Chem. Rev. **87**, 237 (1987).

[5]V. R. Heckman and E. Pollack, Phys. Rev. A **39**, 6154 (1989).

[6]A. A. Wu and F. O. Ellison, J. Chem. Phys. **47**, 1458 (1967).

[7]N. K. Ray, J. Chem. Phys. **52**, 463 (1970).

[8]W. A. Lester, Jr., J. Chem. Phys. **53**, 1511 (1970).

[9]W. A. Lester, Jr., J. Chem. Phys. **54**, 3171 (1971).

[10]W. Kutzelnigg, V. Staemmler, and C. Hoheisel, Chem. Phys. **1**, 27 (1973).

[11]R. C. Raffenetti and K. Ruedenberg, J. Chem. Phys. **59**, 5978 (1973).

[12]E. Kochanski, Chem. Phys. Lett. **28**, 471 (1974).

[13]J. B. Collins, P. v. R. Schleyer, J. S. Binkley, J. A. Pople, and L. Radom, J. Am. Chem. Soc. **98**, 3436 (1976).

[14]Y. A. Borisov and D. G. Musaev, Zh. Strukt. Khim. **23**, 20 (1982).

[15]P. Hobza and P. v. R. Schleyer Chem. Phys. Lett. **105**, 630 (1984).

[16]A. S. Zyubin, A. A. Gorbik, and O. P. Charkin, Zh. Strukt. Khim. **26**, 31 (1985).

[17]B. H. Cardelino, W. H. Eberhardt, and R. F. Borkman, J. Chem. Phys. **84**, 3230 (1986).

[18]D. A. Dixon, J. L. Gole, and A. Komornicki, J. Phys. Chem. **92**, 1378 (1988).

[19]A. Russek, R. Snyder, and R. J. Furlan, Phys. Rev. A **39**, 6158 (1989).

[20]C. H. Wu, J. Chem. Phys. **71**, 783 (1979). It should be noted that in order to arrive at the binding energy of 27.2 kJ mol^{-1} the ionization potential for LiH_2 of 6.14 eV was used. There is some conjecture in the literature (See Ref. 15) that this value is erroneous.

[21]R. K. Nesbet, T. L. Barr, and E. R. Davidson, Chem. Phys. Lett. **4**, 203 (1969).

[22]A. K. Q. Siu and E. R. Davidson, Int. J. Quantum Chem. **4**, 223 (1970).

[23]W. A. Lester, Jr. and J. Schaefer, J. Chem. Phys. **59**, 3676 (1973).

[24]J. P. Toennies, Chem. Soc. Rev. **3**, 407 (1974).

[25]J. Schaefer and W. A. Lester, Jr., J. Chem. Phys. **62**, 1913 (1975).

[26]D. Secrest, in *Atom-Molecule Collision Theory,* edited by R. B. Bernstein (Plenum, New York, 1979).

[27]P. G. Burton, E. I. von Nagy-Felsobuki, and G. Doherty, Chem. Phys. Lett. **104**, 323 (1984).

[28]P. G. Burton, E. I. von Nagy-Felsobuki, G. Doherty, and M. Hamilton, Chem. Phys. **83**, 83 (1984).

[29]P. G. Burton, E. I. von Nagy-Felsobuki, G. Doherty, and M. Hamilton, Mol. Phys. **55**, 527 (1985).

[30]G. Doherty, M. Hamilton, P. G. Burton, and E. I. von Nagy-Felsobuki, Aust. J. Phys. **39**, 749 (1986).

[31]P. G. Burton and E. I. von Nagy-Felsobuki, Chem. Aust. **55**, 408 (1988).

[32]S. J. Dunne, D. J. Searles, and E. I. von Nagy-Felsobuki, Spectrochim. Acta A **43**, 699 (1987).

[33]D. J. Searles, S. J. Dunne, and E. I. von Nagy-Felsobuki, Spectrochim. Acta A **44**, 505 (1988).

[34]D. J. Searles and E. I. von Nagy-Felsobuki, Aust. J. Chem. **42**, 737 (1989).

[35]G. D. Carney, S. R. Langhoff, and L. A. Curtiss, J. Chem. Phys. **66**, 3724 (1977).

[36]D. O. Harris, G. G. Engerholm, and W. D. Gwinn, J. Chem. Phys. **43**, 1515 (1965).

[37]M. J. Frisch, J. S. Binkley, H. B. Schlegel, K. Ragavachan, C. F. Melius, R. Martin, J. J. P. Stewart, F. W. Bohrowicz, C. M. Pohlfing, L. R. Kahn, D. J. DeFrees, R. Seeger, R. A. Whiteside, D. J. Fox, E. M. Fluder, and J. A. Pople, GAUSSIAN 86, 1984, Garnegie-Mellon Quantum Chemistry Publishing Unit, Pittsburgh, PA.

[38]W. H. Gerber and E. Schumacher, J. Chem. Phys. **69**, 1692 (1978).

[39]C. E. Dykstra and W. C. Swope, J. Chem. Phys. **70**, 1 (1979).

[40]W. Kolos and L. Wolniewicz, J. Chem. Phys. **49**, 404 (1968).

[41]C. C. J. Roothaan, L. M. Sachs, and A. W. Weiss, Rev. Mod. Phys. **32**, 186 (1960).

[42]See AIP document No. PAPS PLRAA-43-3365-05 for five pages of discrete CISD potential-energy data. Order by PAPS number and journal reference from American Institute of Physics, Physics Auxiliary Publication Service, 335 East 45th Street, New York, NY 10017. The prepaid price is $1.50 for a microfiche, and $5.00 for photocopies. Airmail addi-

tional. Make checks payable to the American Institute of Physics.
[43]J. L. Dunham, Phys. Rev. **41**, 721 (1932).
[44]G. Simons, R. G. Parr, and J. M. Finlan, J. Chem. Phys. **59**, 3229 (1973).
[45]J. F. Ogilvie, Proc. R. Soc. London Ser. A **378**, 287 (1981).
[46]K. D. Jordan, J. L. Kinsey, and R. Silbey, J. Chem. Phys. **61**, 911 (1974).
[47]V. S. Jorish and N. B. Scherbak, Chem. Phys. Lett. **67**, 160 (1979).
[48]A. Pardo, J. J. Camacho, and J. M. L. Poyato, Chem. Phys. Lett. **131**, 490 (1986).